NASA/TM—2010-216935

Grain Boundary Engineering the Mechanical Properties of Allvac 718Plus™ Superalloy

Timothy P. Gabb and Jack Telesman
Glenn Research Center, Cleveland, Ohio

Anita Garg
University of Toledo, Toledo, Ohio

Peter Lin, Virgil Provenzano, Robert Heard, and Herbert M. Miller
Integran Technologies USA Inc., Pittsburgh, Pennsylvania

December 2010

NASA STI Program . . . in Profile

Since its founding, NASA has been dedicated to the advancement of aeronautics and space science. The NASA Scientific and Technical Information (STI) program plays a key part in helping NASA maintain this important role.

The NASA STI Program operates under the auspices of the Agency Chief Information Officer. It collects, organizes, provides for archiving, and disseminates NASA's STI. The NASA STI program provides access to the NASA Aeronautics and Space Database and its public interface, the NASA Technical Reports Server, thus providing one of the largest collections of aeronautical and space science STI in the world. Results are published in both non-NASA channels and by NASA in the NASA STI Report Series, which includes the following report types:

- TECHNICAL PUBLICATION. Reports of completed research or a major significant phase of research that present the results of NASA programs and include extensive data or theoretical analysis. Includes compilations of significant scientific and technical data and information deemed to be of continuing reference value. NASA counterpart of peer-reviewed formal professional papers but has less stringent limitations on manuscript length and extent of graphic presentations.

- TECHNICAL MEMORANDUM. Scientific and technical findings that are preliminary or of specialized interest, e.g., quick release reports, working papers, and bibliographies that contain minimal annotation. Does not contain extensive analysis.

- CONTRACTOR REPORT. Scientific and technical findings by NASA-sponsored contractors and grantees.

- CONFERENCE PUBLICATION. Collected papers from scientific and technical conferences, symposia, seminars, or other meetings sponsored or cosponsored by NASA.

- SPECIAL PUBLICATION. Scientific, technical, or historical information from NASA programs, projects, and missions, often concerned with subjects having substantial public interest.

- TECHNICAL TRANSLATION. English-language translations of foreign scientific and technical material pertinent to NASA's mission.

Specialized services also include creating custom thesauri, building customized databases, organizing and publishing research results.

For more information about the NASA STI program, see the following:

- Access the NASA STI program home page at *http://www.sti.nasa.gov*

- E-mail your question via the Internet to *help@sti.nasa.gov*

- Fax your question to the NASA STI Help Desk at 443–757–5803

- Telephone the NASA STI Help Desk at 443–757–5802

- Write to:
  NASA Center for AeroSpace Information (CASI)
  7115 Standard Drive
  Hanover, MD 21076–1320

NASA/TM—2010-216935

Grain Boundary Engineering the Mechanical Properties of Allvac 718Plus™ Superalloy

Timothy P. Gabb and Jack Telesman
Glenn Research Center, Cleveland, Ohio

Anita Garg
University of Toledo, Toledo, Ohio

Peter Lin, Virgil Provenzano, Robert Heard, and Herbert M. Miller
Integran Technologies USA Inc., Pittsburgh, Pennsylvania

Prepared for the
7th International Symposium on Superalloy 718 and Derivatives
sponsored by the Minerals, Metals and Materials Society (TMS)
Pittsburgh, Pennsylvania, October 10–13, 2010

National Aeronautics and
Space Administration

Glenn Research Center
Cleveland, Ohio 44135

December 2010

Level of Review: This material has been technically reviewed by technical management.

Available from

NASA Center for Aerospace Information
7115 Standard Drive
Hanover, MD 21076–1320

National Technical Information Service
5301 Shawnee Road
Alexandria, VA 22312

Available electronically at http://gltrs.grc.nasa.gov

Grain Boundary Engineering the Mechanical Properties of Allvac 718Plus™ Superalloy

Timothy P. Gabb and Jack Telesman
National Aeronautics and Space Administration
Glenn Research Center
Cleveland, Ohio 44135

Anita Garg
University of Toledo
Toledo, Ohio 43606

Peter Lin, Virgil Provenzano, Robert Heard, and Herbert M. Miller
Integran Technologies USA Inc.
Pittsburgh, Pennsylvania 15241

Abstract

Grain Boundary Engineering (GBE) can enhance the population of structurally-ordered "low Σ" Coincidence Site Lattice (CSL) grain boundaries in the microstructure. In some alloys, these "special" grain boundaries have been reported to improve overall resistance to corrosion, oxidation, and creep resistance. Such improvements could be quite beneficial for superalloys, especially in conditions which encourage damage and cracking at grain boundaries. Therefore, the effects of GBE processing on high-temperature mechanical properties of the cast and wrought superalloy Allvac 718Plus (Allvac ATI) were screened. Bar sections were subjected to varied GBE processing, and then consistently heat treated, machined, and tested at 650 °C. Creep, tensile stress relaxation, and dwell fatigue crack growth tests were performed. The influences of GBE processing on microstructure, mechanical properties, and associated failure modes are discussed.

Introduction

Cast and wrought superalloys were designed to have strength and creep resistance at moderately high temperatures extending up to 600 °C, for many applications in propulsion, energy, and petrochemical industries. Strengthening precipitate content and refractory element levels have been carefully balanced to allow cold working, hot working, and joining, without cracking or other severe damage. Recently developed cast and wrought superalloys such as Allvac 718Plus (Allvac ATI) and Haynes 282 (Haynes International) have retained these capabilities, while extending mechanical property capabilities to over 650 °C (Refs. 1 and 2). However, as temperatures increase to this level, time-dependent failure modes including creep, dwell fatigue cracking at notches, and dwell fatigue crack growth can limit life in some applications, often due to intergranular cracking (Ref. 3).

In the presence of dwells, fatigue cracks often initiate and grow at surface grain boundaries. This intergranular cracking is environment related, and therefore not easily suppressed unless the environment is changed (Refs. 4 and 5). However, grain size and associated grain boundary characteristics have been found to influence this intergranular crack growth rates in air (Refs. 6, 7, and 8). For materials of fixed grain size, the response can also be strongly influenced by heat treatments that vary the size and volume fraction of strengthening precipitates, thereby altering the balance of mechanical properties that control stresses at cracks (Refs. 9 and 10). Heat treatments using fast solution quenches and low temperature ages can produce refined secondary and tertiary γ' precipitate sizes that maximize strength and creep resistance, but allow high peak stresses at cracks to impair resistance to dwell fatigue crack growth.

Alternative heat treatments using slower solution quenches and higher temperature ages can produce larger secondary and tertiary γ′ precipitate sizes that reduce strength and creep resistance, but give lower peak stresses at cracks to improve resistance to dwell fatigue crack growth. Alloys like 718Plus can be given heat treatments to promote the formation of coarse δ phase at the grain boundaries (10). This δ phase content comes at the expense of γ′ precipitate phase content (Ref. 1) and therefore reduces strength and creep resistance, but can improve dwell crack growth resistance. In summary, the particular trade in tensile and creep strength versus dwell crack growth is common to many disk superalloys, and can limit disk designs.

Low CSL grain boundaries have been reported to be more resistant to oxidation, corrosion, and creep in some superalloys (Refs. 11, 12, and 13). Therefore, increasing the fraction of such special grain boundaries (i.e., Fsp) in disk superalloys could influence the balances and trades of mechanical properties available, to potentially improve resistance to crack growth during fatigue with dwells. The objective of this study was to screen the influence of grain boundary engineering processing on the microstructure and high temperature mechanical properties of a disk superalloy, in search of an improved balance of dwell fatigue crack growth with other mechanical properties. Selected samples of 718Plus superalloy were given GBE treatments to increase the fraction of low CSL grain boundaries. Several heat treatments were also consistently applied, to vary grain size and precipitate size in samples with and without prior GBE processing. Specimens were then subjected to tensile stress relaxation, creep, and dwell fatigue crack growth tests. Properties and failure modes were then compared.

Materials and Procedure

Allvac 718Plus was obtained from ATI Allvac as a hot rolled, annealed bar of 3.5 cm diameter, having a composition of 1.46Al, 0.005B, 0.21C, 8.99Co, 0.01Cu, 17.79Cr, 9.53Fe, 2.69Mo, 0.05Mn, 5.47Nb, 0.008P, 0.06Si, 0.0003S, 0.75Ti, 0.03V, 1.02W, bal. Ni (weight percent) and trace impurities. Grain boundary engineering was performed by repetitive cycles of cold rolling with short annealing heat treatments. The processing conditions of the six cases examined here are listed in Table 1. A full description of the GBE processing and resulting characteristics, including the "GI" and "GII" processes selected to produce preferred grain boundaries in this work, is in an accompanying paper in these proceedings (Ref. 14). Both NG and NGD cases had No GBE processing, but NGD had a Delta (δ) phase heat treatment of 930 °C/4 h/air cool. The GI case received the "GI" GBEI process. The GIP case received the "GI" process, then a Post solution cold rolling deformation reduction of less than 5 percent. The GIIP case followed a similar path, but received the alternative "GII" GBEII process and the Post solution cold rolling reduction. The GIPD case received the "GI" process, a Post solution cold-rolling deformation reduction of less than 5 percent, then the Delta (δ) heat treatment. After GBE processing, all GBE and non-GBE processed blanks, which were 3 cm wide, 1.5 cm thick, and 5.1 cm long, were given an identical solution heat treatment above the estimated γ′ solvus (Ref. 1) of 1025 °C for 5 min., then cooled at a rate of 60 to 70 °C/min to below 800 °C. All blanks were finally given a final two-step aging heat treatment of 788 °C/8 h+38C/min cool+649 °C/8 h/air cool to age the γ′ precipitates. For each selected material case, blanks of the same dimensions received the same final solution heat treatment, controlled quench rate, and final two-step aging heat treatment, to isolate effects of GBE processing and the δ heat treatment on microstructure and mechanical properties.

Tensile stress relaxation, creep rupture, and dwell fatigue crack growth tests were performed at 650 °C. Tensile stress relaxation tests were performed on specimens having a gage diameter of 0.4 cm and gage length of 2 cm in a uniaxial test machine employing a resistance heating furnace and axial extensometer. The tests were performed in general accordance with the tensile testing standard ASTM E21, using an initial test segment with strain increased at a uniform rate of 0.5 percent/min. However, the tests were stopped at 1 percent strain and held for 100 h, to measure relaxation of stress as a function of time. The tensile tests were then continued to failure, at a uniform displacement rate of 1 mm/min.

Creep tests were performed on specimens of the same dimensions at Metcut Research Associates in general accordance with ASTM E139, using uniaxial lever arm constant load creep frames with resistance heating furnaces and gage-mounted extensometers. Tests at an applied stress of 690 MPa were interrupted after attaining at least 0.5 percent creep strain. The samples were measured to verify elongation, and later continued to rupture at NASA GRC using uniaxial lever arm constant load creep frames with resistance heating furnaces and displacement gages for monitoring creep strain.

Fatigue crack growth specimens were machined with a rectangular gage section 1 cm wide and 0.46 cm thick, having a surface flaw on one side of the gage section about 0.356 mm wide and 0.178 mm deep, produced by electro-discharge machining (Ref. 15). The fatigue crack growth specimens were tested at NASA GRC in general accordance with ASTM E647. Tests were performed in a closed-loop servo-hydraulic test machine using resistance heating, with potential drop measurement of crack growth. Pre-cracking was performed at room temperature, then tests were performed at 650 °C using a maximum stress of 621 MPa, stress ratio of 0.5, and dwell time of 90 s at maximum stress in each cycle.

Fracture surfaces of representative specimens were evaluated by scanning electron microscopy (SEM). Cracking modes and grain sizes were also examined on metallographically-prepared sections for selected specimens. Grain sizes were determined on metallographically-prepared samples according to ASTM E112 using linear intercept grids on optical images. An EDAX Inc. electron back scatter orientation imaging system was used with TSL software in a field emission scanning electron microscope to determine grain orientation and grain boundary character, as described in Reference 14. Precipitate microstructures were also compared in thin foils using <100> γ/γ' dark field images in a FEI CM200 transmission electron microscope (TEM). At least 150 precipitates were measured within grains for each material condition.

Results and Discussion

Material and Microstructures

Typical grain microstructures from etched metallographic sections of tensile test specimens are shown in Figures 1 to 3. Grain sizes and grain boundary characteristics are summarized in Table 1 (Ref. 14). The six 718Plus conditions had mean linear intercept grain sizes varying from 16 to 30 μm. The percentage of low CSL "special" grain boundaries (Fsp) increased from 35 percent for non-GBE conditions up to 69 percent for the GIIP condition. Twin density increased from 17 percent for non-GBE condition up to 56 percent for the GIIP condition. The enhancement of Σ3 (i.e., twin boundary) content is a key step in GBE, and has been previously observed in many other superalloys (Refs. 11, 13, 16, and 17). Twin boundaries have a CSL of 3, and are therefore counted as low energy CSL boundaries in this accepted methodology and in the present results.

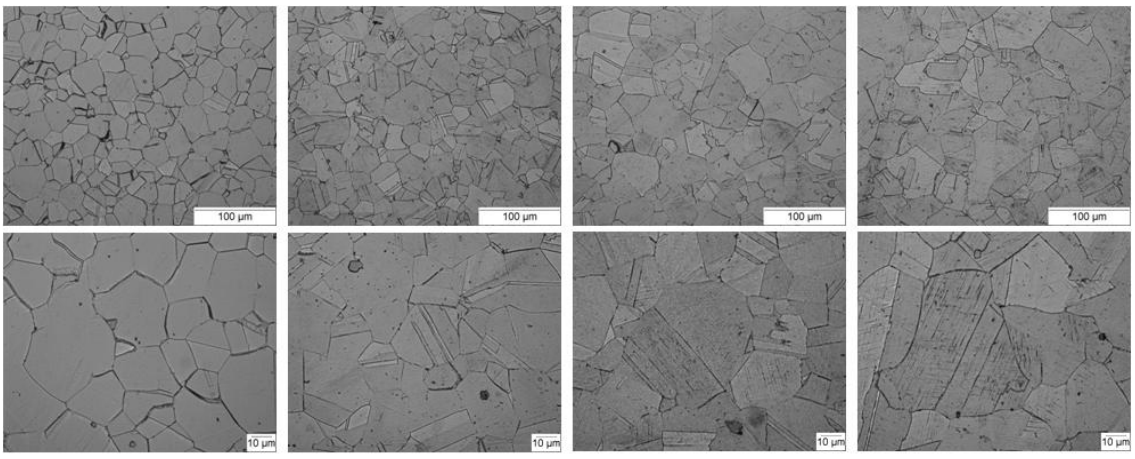

Figure 1.—Optical images of samples given conventional 718Plus heat treatment.

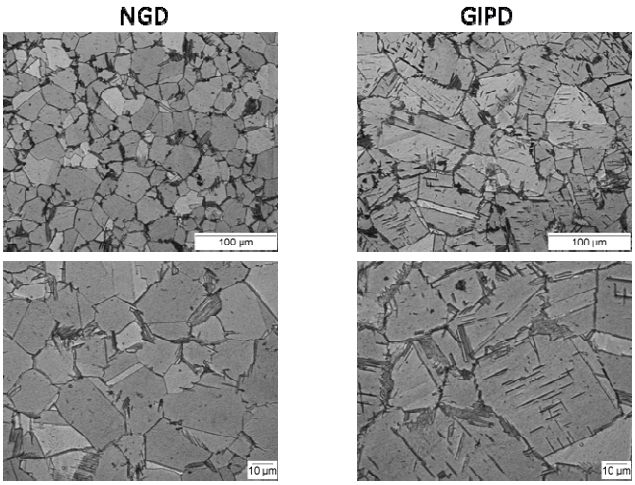

Figure 2.—Optical images of samples given δ heat treatment.

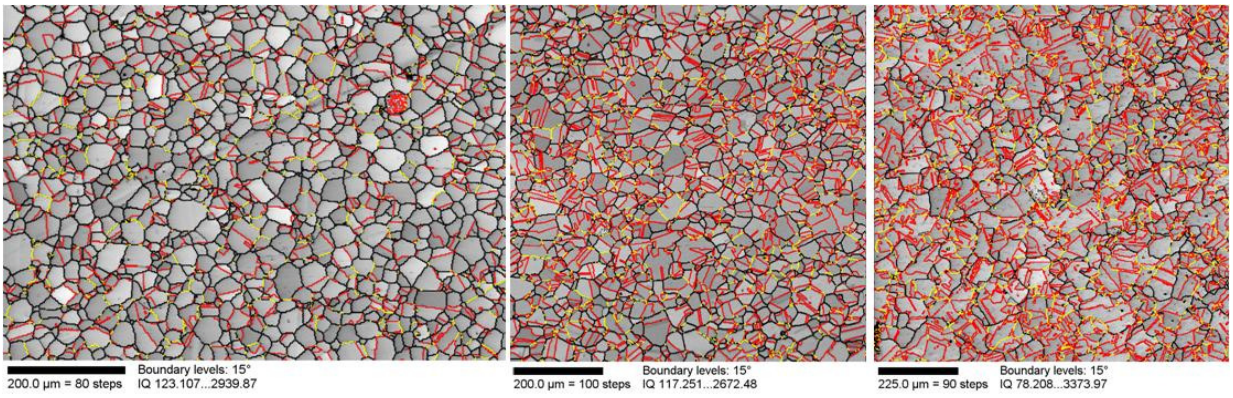

Figure 3.—Representative OIM images of the Allvac 718Plus Alloy in NG (No GBE), GI (GBE I) and GIIP (GBEII, post-solution deformation) conditions showing the increase in the special grain boundaries content following the applied GBE processing. The boundary segments are classified as follows: red lines denote low energy Σ3 grain boundaries, yellow denotes other low Σ(i.e., $3<\Sigma\leq29$) grain boundaries, thick black lines represent general high angle grain boundaries and thin black lines show the positions of the low angle grain boundaries (i.e., Σ1).

TABLE 1.—A SUMMARY OF NOMENCLATURE, PROCESSING HISTORY AND FINAL MICROSTRUCTURAL CHARACTERISTICS FOR THE SIX CASES

Sample Condition	Processing Sequence and Description	Linear Intercept Grain Size (µm)	Twin Density (%)	Fraction of Special Boundaries (Fsp-%)	Mean Fine Gamma Prime Dia. (nm)	Coarse Gamma Prime Dia. (nm)
No GBE (NG)	ΛR → GFHT → ΛHT	16	17	35	34±8	
GBEI (GI)	GBEI → ΛHT	19	45	60	41±11	
GBEI, Post solution deformation (GIP)	GBEI → PD → ΛHT	20	50	59	34±8	
GBEII, Post solution deformation (GIIP)	GBEII → PD → ΛHT	26	56	69	43±9	
No GBE, Delta Heat Treatment (*NGD*)	ΛR → GFHT → DHT → ΛHT	16	24	34	29±7	115±23
GBEI, Post solution deformation, Delta Heat Treatment (*GIPD*)	GBEI → PD → DHT → ΛHT	30	52	64	34±8	134±29

ΛR - Material in the as-received condition
GBEI – GBE with Fsp >60%
GBE II - GBE with the highest Fsp >70%
GFHT - GBE final Heat Treatment
PD – Post solution Deformation
DHT - Delta Heat Treatment: 930°C/4h
ΛHT - 2-stage Λging Heat Treatment: 788°C/8h + -38°C/h + 649°C/8h/ΛC

Precipitate microstructures are compared in the TEM images of Figure 4. Mean secondary γ′ precipitate size moderately increased with GBE for conventionally aged materials, in going from the NG to GI and GIIP conditions. These samples were heat treated identically, so the precipitate size differences were related to GBE and post-solution deformation. Very fine γ″ phase particles, shown in example insets, were observed attached to γ′ precipitates for all cases. However, the size and extent of these γ″ particles appeared comparable among the different conditions. This has been observed in some cases for 718 in the past (18). The δ heat treated conditions (NGD and GIPD) had δ plates often extending from grain boundaries, and similar bimodal γ′ precipitate size distributions for the NGD and GIPD cases, Figure 4(b). Here too, the fine γ′ precipitate size was increased by GBE for the GIPD condition. Compared to NGD, the GIPD condition also had slightly higher δ phase content, with δ plates added within grains along preferred crystallographic planes. This was apparently due to preferential δ phase nucleation at slip bands after plastic deformation, as sometimes observed for 718 (Ref. 19). For all conditions, γ′ precipitates were distributed uniformly within grains, and preferential coarsening or denuding of γ′ precipitates at grain boundaries was not typically observed.

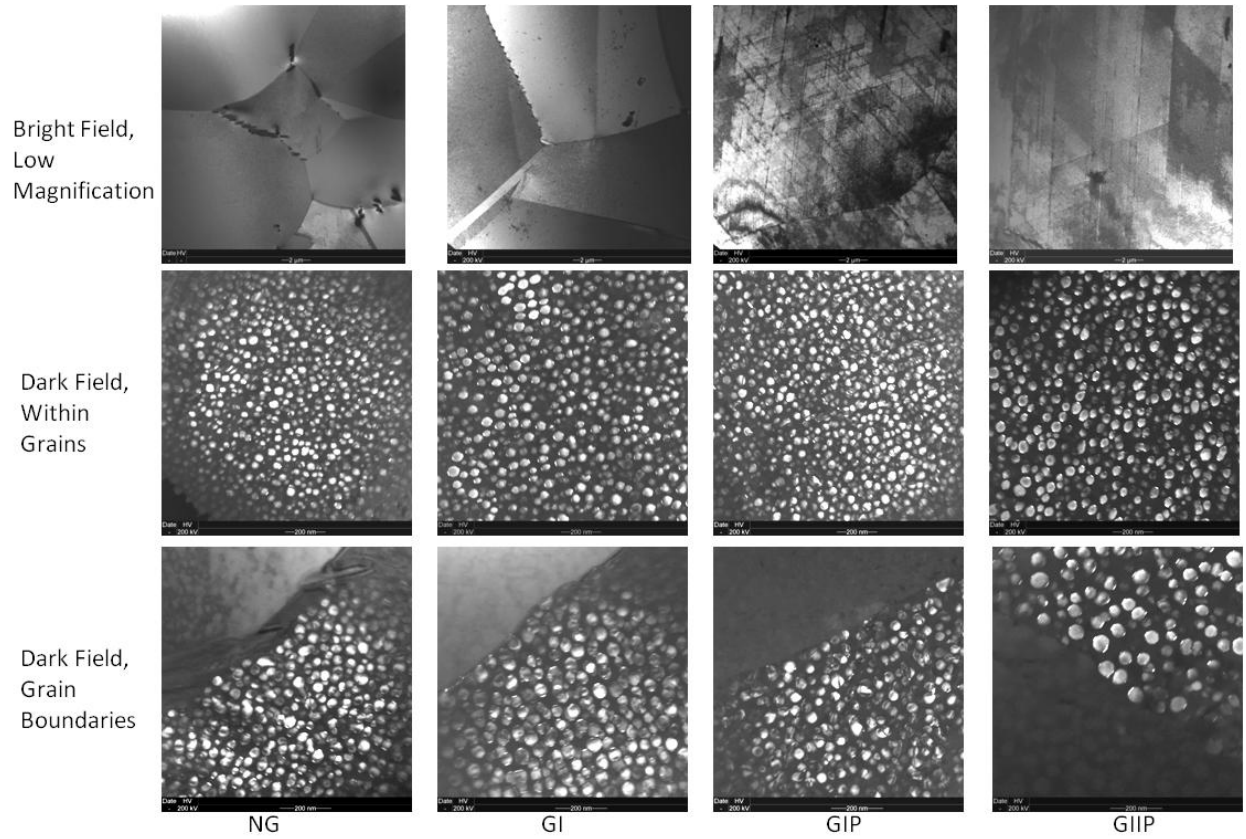

Figure 4(a).—TEM images of cases with conventional 718Plus heat treatment.

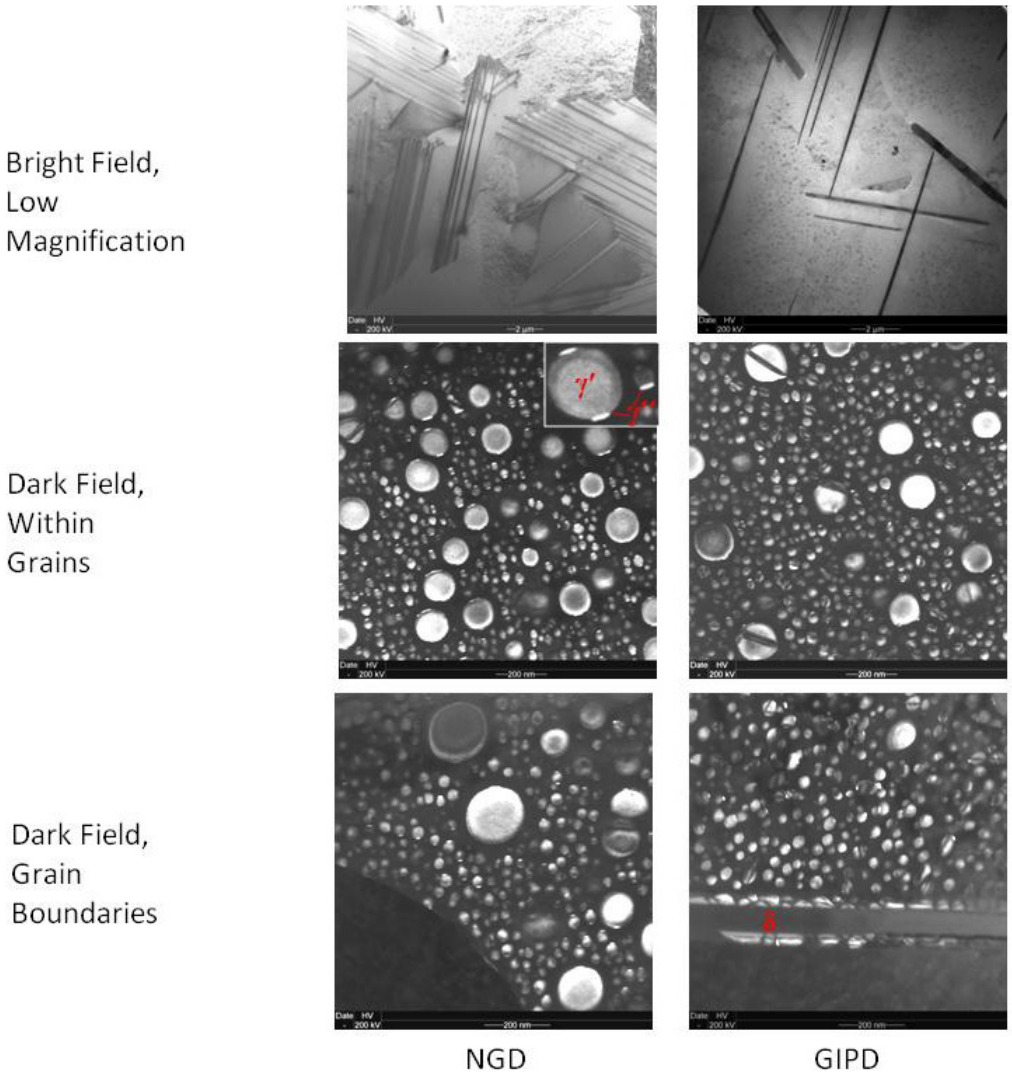

Figure 4(b).—TEM images of cases with δ heat treatment.

Mechanical Response

Tensile.—Typical tensile stress-strain and relaxed stress-time curves are shown in Figure 5, and tensile results are compared in Figure 6. GI samples, which were GBEI processed without the additional cold-rolling deformation step following the final solution treatment, had 9 percent lower mean yield strength than comparative NG samples without the processing. However, GIP and GIIP, which were GBE processed and also given post-solution deformation, had up to 9 percent increased mean yield strength. δ heat treated materials had lower yield strengths than for conventional heat treat conditions, and were less affected by GBE. GBE only increased mean yield strength for condition GIPD about 1 percent over its non-GBE equivalent, NGD. Ultimate strength is also compared for all cases in Figure 6. δ heat treated materials consistently had lower mean ultimate strength than conventionally heat treated materials. Yet, mean ultimate strength was not strongly affected by GBE processing for any heat treatment condition. The δ heat treatment gave increased ductility over the conventional heat treat condition. But GBE did not strongly affect ductility for any heat treatment condition. This indicated that deformation introduced during the cold rolling operations of GBE and sometimes after final solution heat treatments did not "consume" or decrease monotonic tensile ductility.

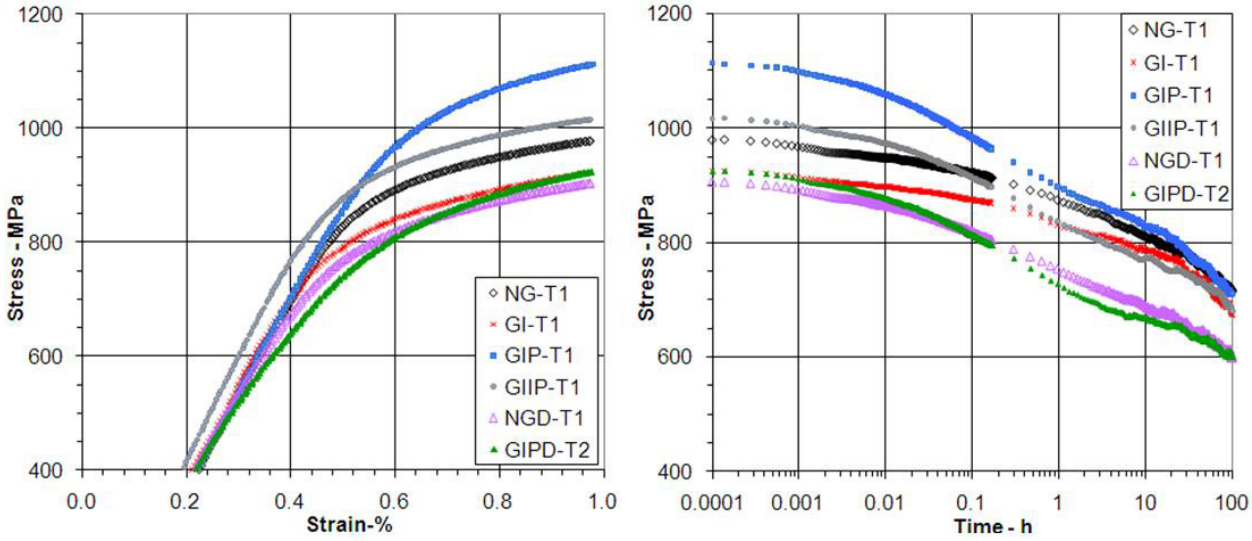

Figure 5.—Typical tensile stress-strain and stress relaxation curves.

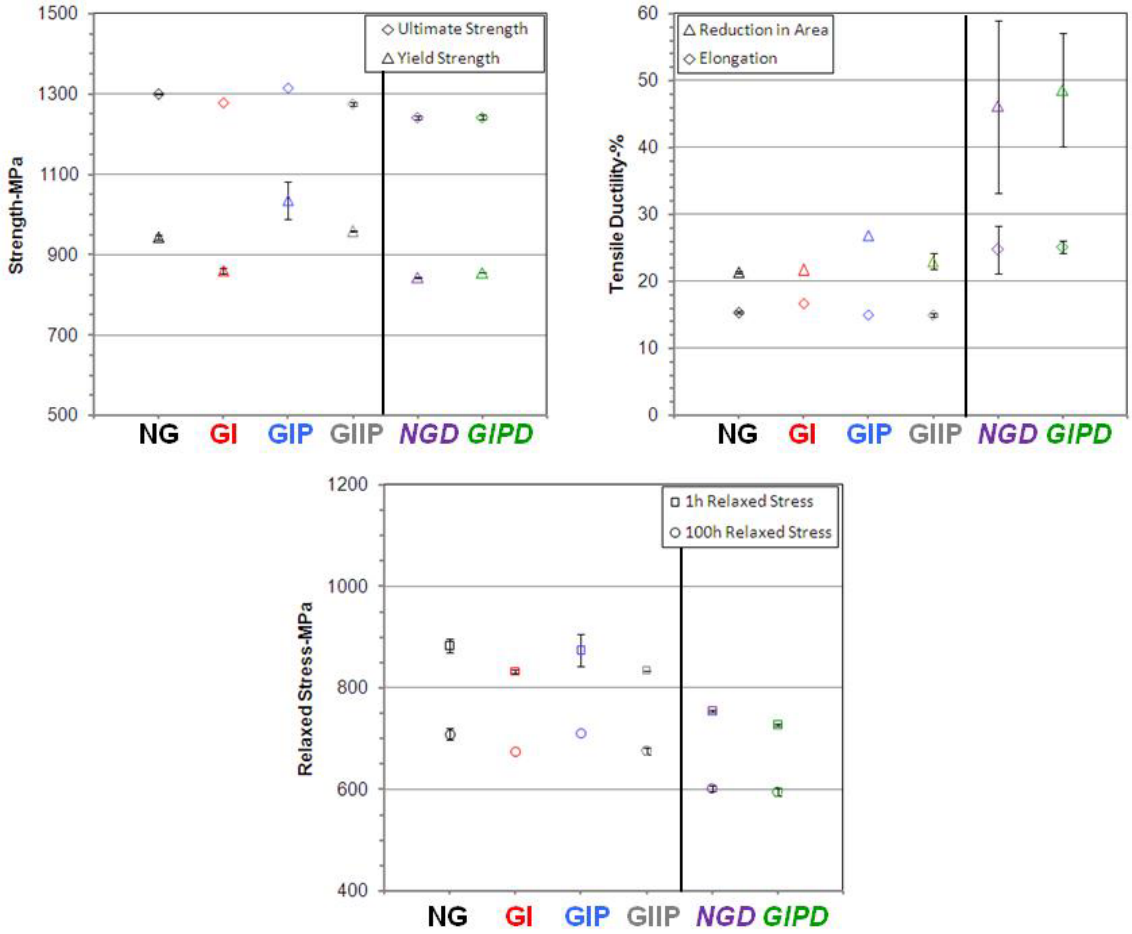

Figure 6.—Tensile strengths, ductilities, and relaxed stresses, with error bars indicating ± one standard deviation.

Stresses relaxed nearly 300 MPa over 100 h of stress relaxation for both heat treat conditions in materials without GBE processing, NG and NGD, as shown in Figure 6. Equivalent samples given GBE with post-solution deformation (GIP and GIIP) allowed increased stress relaxation, so that in spite of their increased yield strength, final relaxed stress at 100 h was comparable. This resulted in final relaxed stresses near 700 MPa for conventional heat treat conditions, and near 600 MPa for δ heat treat conditions. The largest relaxation in stress occurred for the GIP samples, 375 MPa. However, the GI samples having only baseline GBEI processing were unique, combining reduced yield strength with reduced stress relaxation of just 187 MPa. Final relaxed stress for this case matched those for the δ heat treated condition, near 600 MPa. This was strikingly different from GIP samples, which had post-solution deformation after the same GBEI processing.

Tensile fractures were dominated by conventional ductile shear near the specimen surface and microvoid coalescence in the center. However, one or more intergranular surface cracks also initiated along the surface, and influenced failures for most tensile specimens, Figure 7. Only the GIPD condition had no intergranular cracks on the fracture surface.

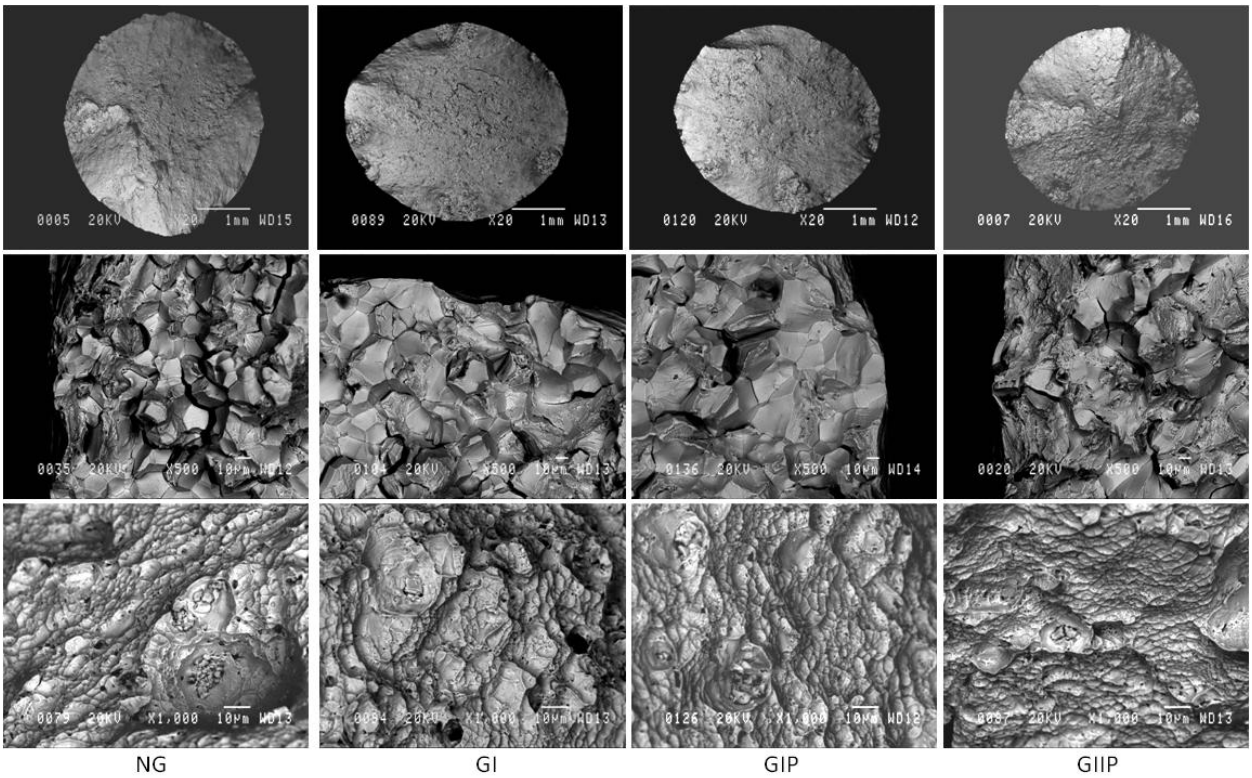

Figure 7(a).—Typical tensile fracture surfaces, intergranular edge cracks, and central overload regions, for cases with conventional aging heat treatment.

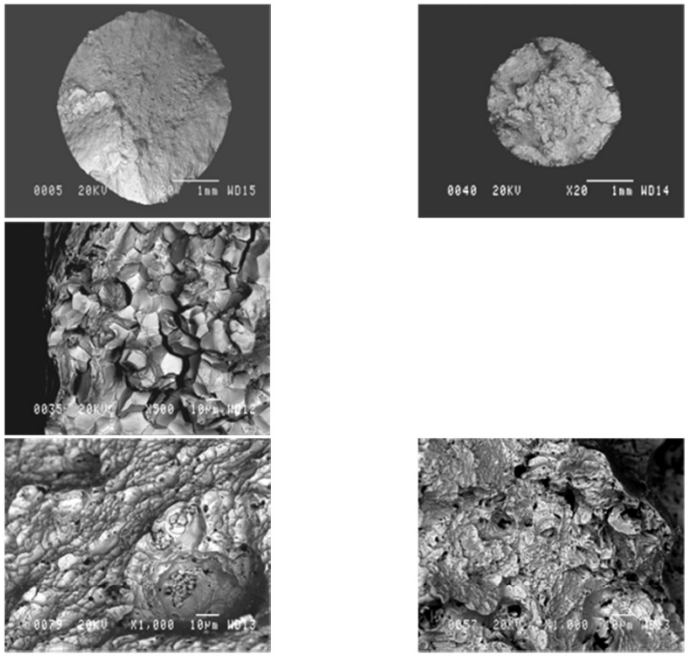

Figure 7(b).—Typical tensile fracture surfaces, intergranular edge cracks, and central overload regions, for δ heat treatment.

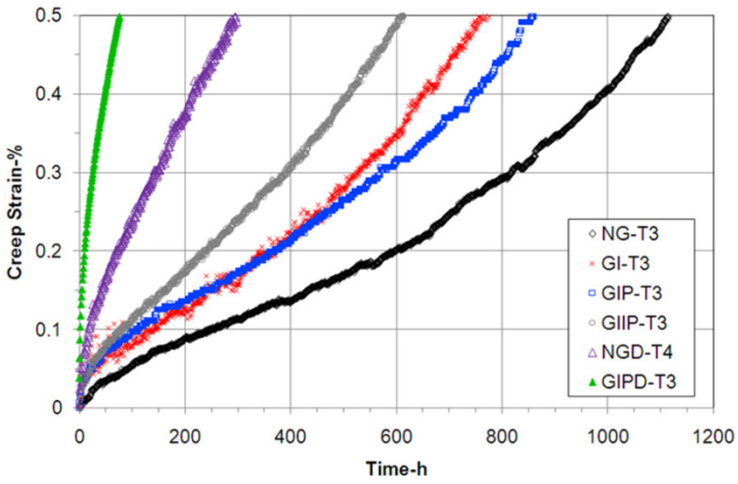

Figure 8.—Typical creep curves for tests at 650 °C/690 MPa.

Creep.—Typical creep-time curves are shown in Figure 8, and creep results are compared in Figure 9. The δ heat treatment gave greatly increased primary creep and reduced creep resistance over the conventional heat treat condition, reducing time to 0.5 percent creep by about 70 percent. GBE further increased primary creep extent and reduced creep times for both δ and conventional heat treatment conditions. Unlike stress relaxation response, creep responses for GI and GIP conditions were comparable. Yet, mean rupture lives were similar for most conditions, and did not rank in this order. Only the GIPD condition had higher rupture mean life than all other conditions, in spite of its most rapid primary creep. The associated rupture ductilities are also compared in Figure 9. The NG condition had lowest and GIPD condition had highest mean ductilities of all conditions studied. Therefore, deformation introduced during the various cold rolling steps also did not appear to result in lower rupture ductility.

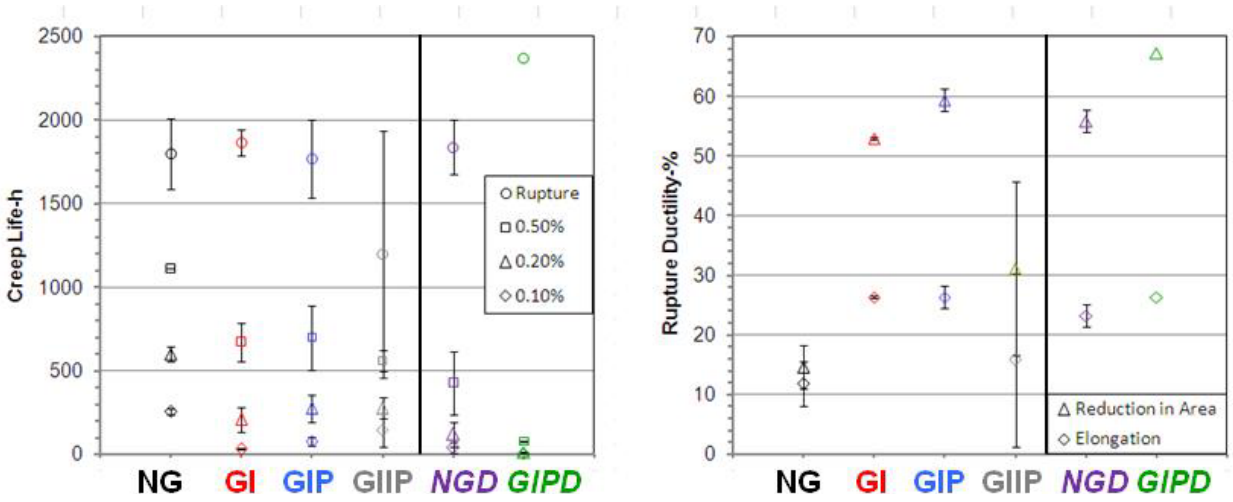

Figure 9.—Creep rupture lives and ductilities, with error bars indicating ± one standard deviation.

Microvoid coalescence again occurred in the specimen centers for creep rupture specimens. But larger intergranular surface cracks were observed for most conditions, Figure 10. These surface cracks were more oxidized than the center regions, indicating that the surface cracks were open longer and likely initiated failures. Again, the GIPD condition had no intergranular surface cracks on the fracture surface.

Dwell fatigue crack growth: The varied material conditions significantly affected the dwell crack growth rate response producing a range of near 10x in crack growth rates, and also altered the crack growth slope for some of the GBE conditions, Figure 11. In addition to the GBE process, the δ heat treatment in itself altered the crack growth rates by lowering them approximately 2x in comparison to the conventional non-GBE heat treat condition NG. GBEI processing with post-solution deformation further reduced dwell crack growth rates by at least 3x for the δ heat treatment condition GIPD, especially at low stress intensities. However, results were mixed for conventional heat treat conditions. The GI condition had a slight reduction in dwell crack growth rate, yet the GIP condition having the same GBEI processing combined with post- solution deformation did not. The GIIP condition with the enhanced GBEII processing and post- solution deformation had dwell crack growth rates reduced by 3 to 10x, especially at low stress intensities. Overall, it appeared GBE could reduce dwell crack growth rates for both conventional and δ heat treated materials. However, the response of conventionally heat treated materials appeared to be sensitive to the GBE processing history.

The extent of intergranular cracking varied significantly among the material conditions, Figure 12, and was influenced by GBE as well as heat treatment. Among conventionally heat treated conditions, the NG condition with no GBE processing had nearly 100 percent intergranular cracking. The GI and GIP conditions appeared to have near 90 percent intergranular cracking, with scattered transgranular grain failures. A lower proportion of near 75 percent intergranular cracking was apparent for the GIIP condition, with transgranular grain failures more often observed. δ heat treated conditions had less intergranular cracking. A near evenly mixed mode of 50 percent intergranular and 50 percent transgranular cracking was apparent for the NGD condition. Finally, the GIPD condition had approximately 75 percent transgranular and 25 percent intergranular cracking.

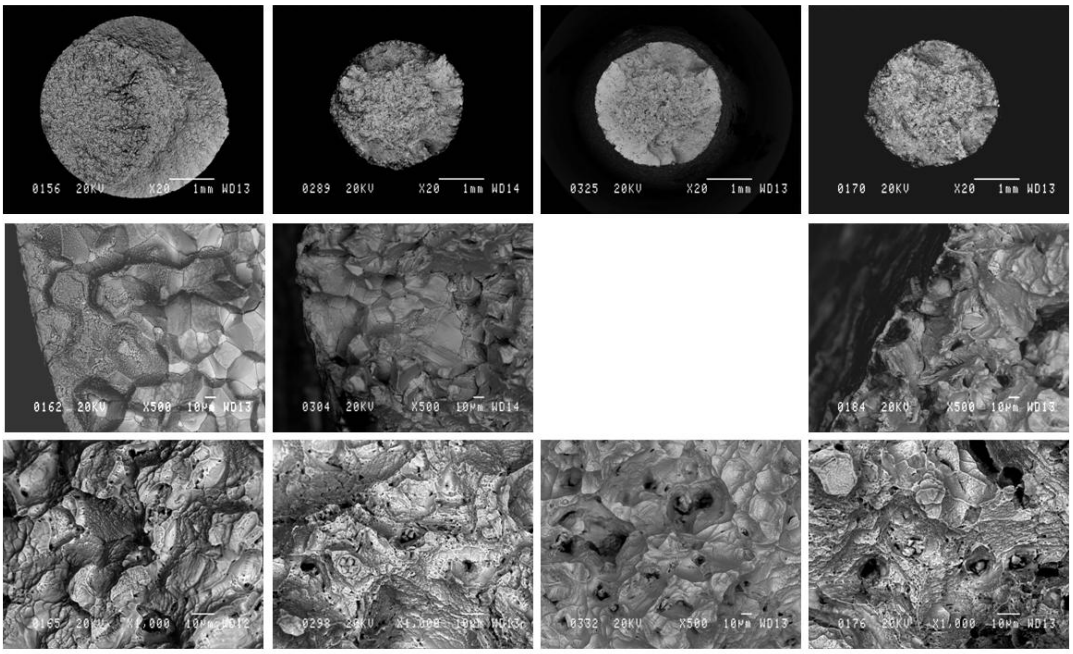

Figure 10(a).—Typical creep rupture fracture surfaces, intergranular edge cracks, and central overload regions, for cases with conventional heat treatment.

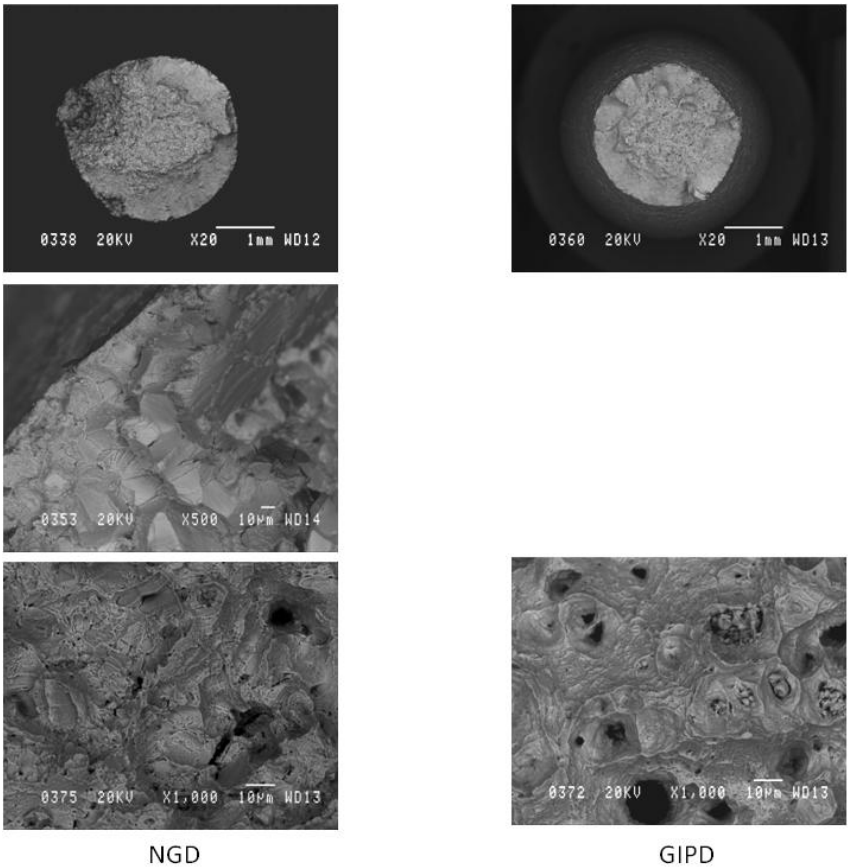

Figure 10(b).—Typical creep rupture fracture surfaces, intergranular edge cracks, and central overload regions, for cases with δ heat treatment.

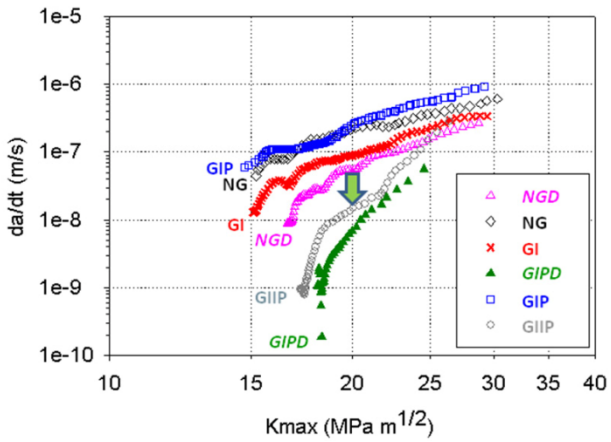

Figure 11.—Typical 90s dwell fatigue crack growth rates versus maximum stress intensity at 650 °C.

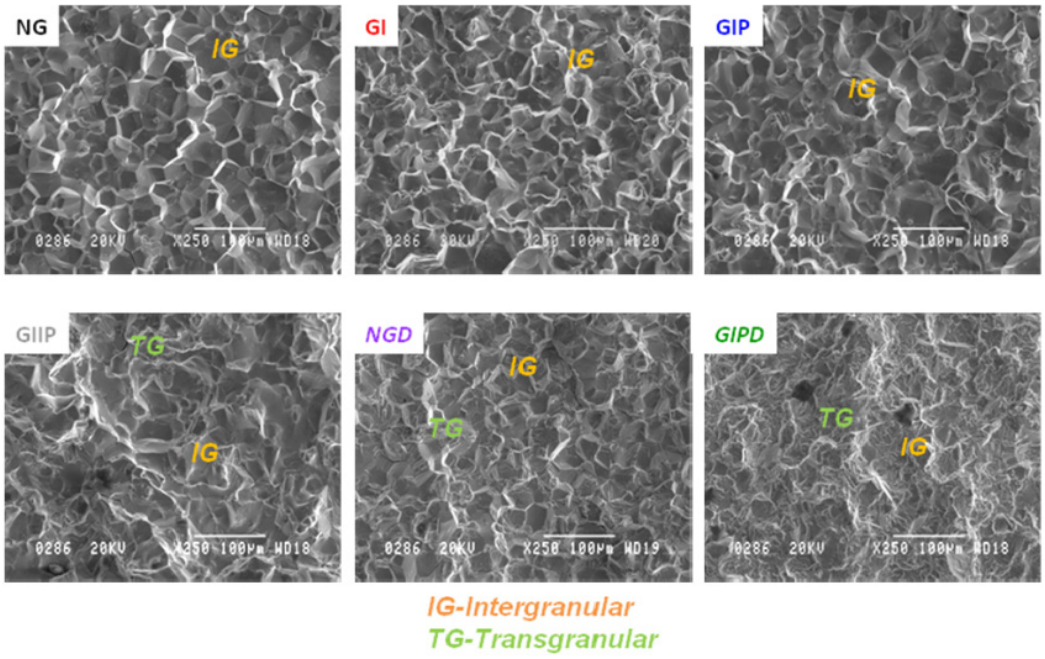

Figure 12.—Typical dwell fatigue crack growth surfaces.

Microstructure-Property Relationships

For the material conditions examined, GBE increased the proportion of preferred grain boundaries and twins, and in some cases, corresponding grain sizes were also affected. GBE also influenced γ′ and δ phase morphologies. All these changes need be considered in relating GBE processing to observed microstructures and mechanical properties.

GBE-Microstructure.—The bimodal population of γ′ precipitates observed for the NGD and GIPD cases can be explained by comparing the δ heat treatment and γ′ phase solvus temperatures. The δ heat treatment temperature of 930 °C is below the estimated γ′ phase solvus temperature of 1065 °C (Ref. 1), therefore a small fraction of the existing γ′ precipitates would not dissolve, but instead coarsen appreciably during the δ heat treatment. The dissolved γ′ phase fraction would then re-precipitate and grow to finer sizes during the subsequent quench and aging heat treatments, giving the bimodal population.

Both conventional and δ heat treated cases received the same final solution heat treatments above the γ′ solvus, controlled quench rate, and final aging heat treatments. Yet, mean γ′ size often increased for GBE processed materials in each case. This indicates GBE processing in some way affected subsequent precipitate nucleation, growth, and coarsening, perhaps driven by remnant cold work not fully annealed in the short 5 min solution treatments. Combining GBE with post-solution cold work apparently further enhanced these effects, evident in comparing the microstructures for GI and GIIP conditions, Figure 4. Curiously, the enhancement was not observed for the GIP condition. Further experimentation would be necessary to determine exactly how this enhancement varies and occurs. Additional δ phase also precipitated within grains due to GBE processing, observed for the GIPD condition. This is consistent with reported observations in studies of 718, which showed that δ phase preferentially nucleates at slip bands produced by plastic deformation (Ref. 19).

Microstructure-Properties.—The relationships between microstructure and mechanical properties are separately considered in Figures 13 to 15. Mechanical properties are shown versus special grain boundary content in Figure 13. Stress relaxation significantly increased, while creep time and dwell fatigue crack growth rate significantly decreased with special grain boundary content. Properties are shown versus grain size in Figure 14. Dwell fatigue crack growth rate strongly correlated with grain size. Strength, relaxed stress, and creep time did not clearly correlate with only grain size. As indicated, post-solution deformation appeared to influence these properties, and could help explain the lack of clear grain size dependence here. Mechanical properties are shown as functions of fine γ′ size in Figure 15. Stress relaxation significantly increased and dwell fatigue crack growth rate correspondingly decreased with fine γ′ size.

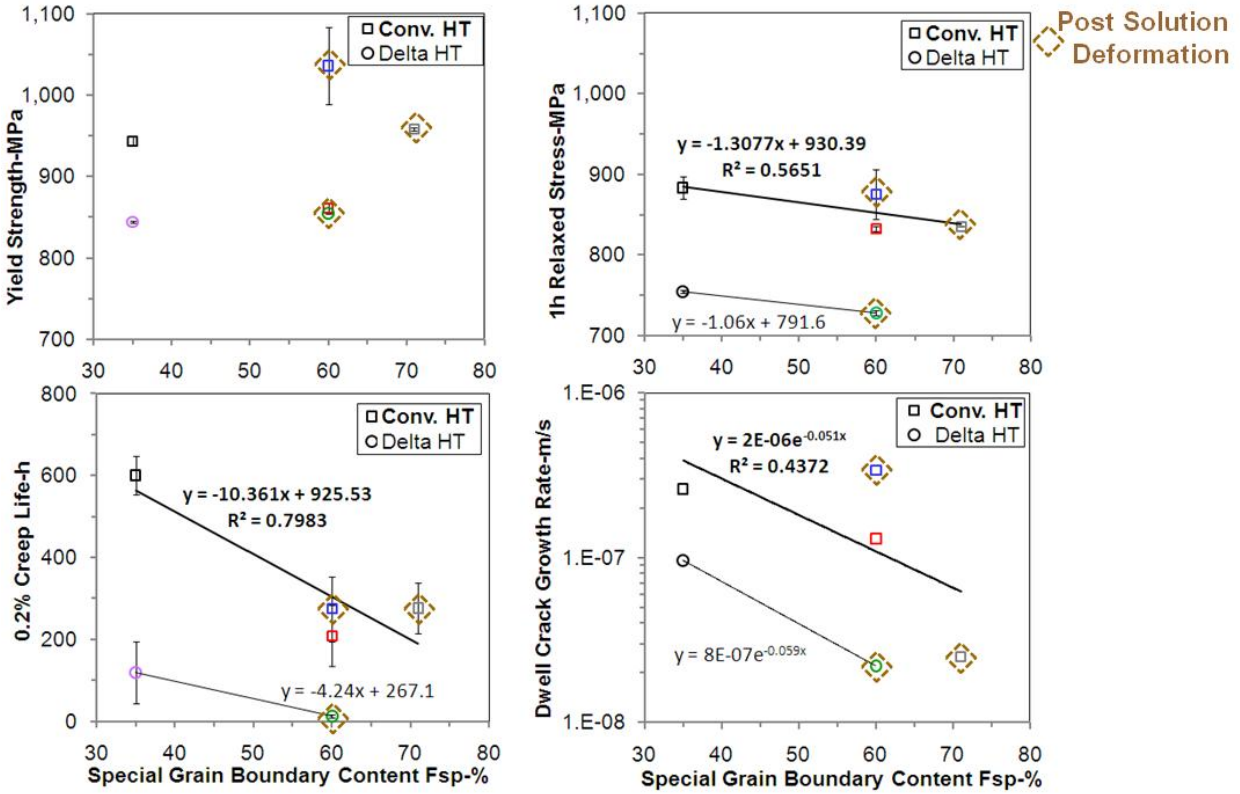

Figure 13.—Mechanical properties versus special grain boundary content.

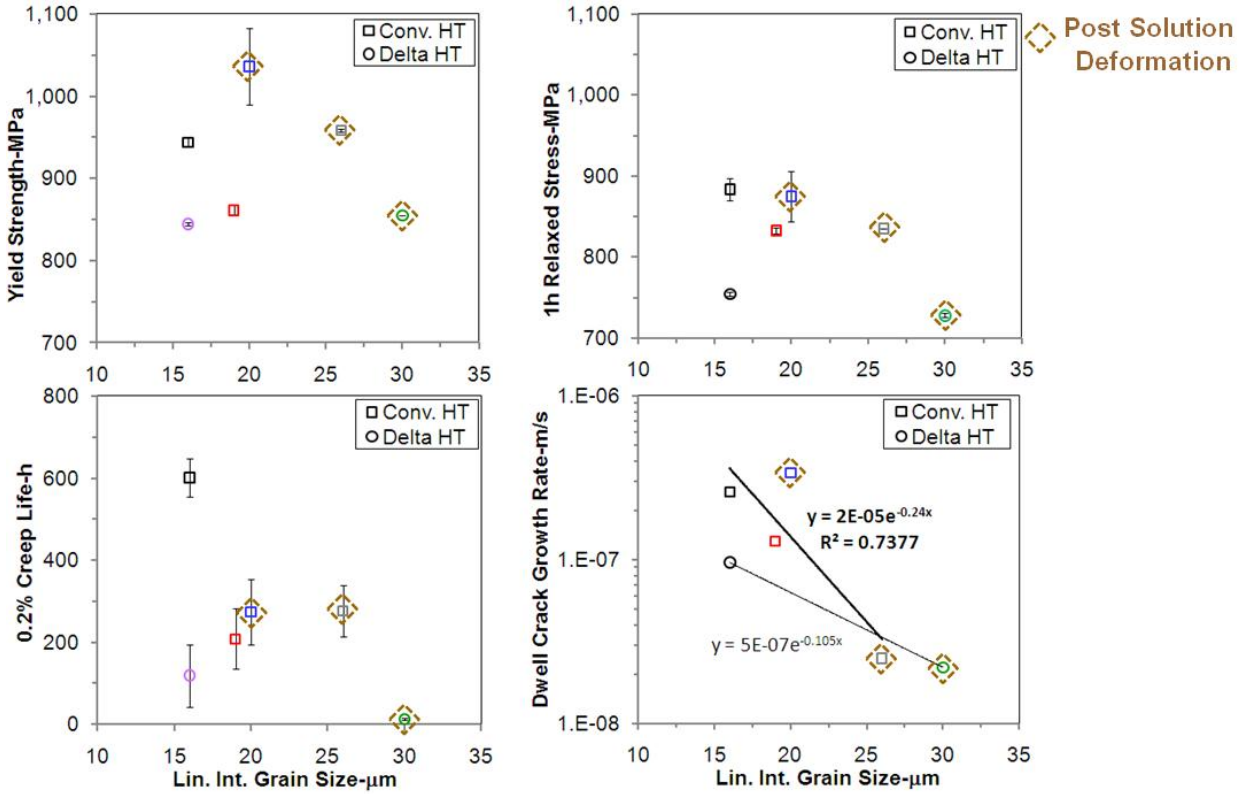

Figure 14.—Mechanical properties versus linear intercept grain size.

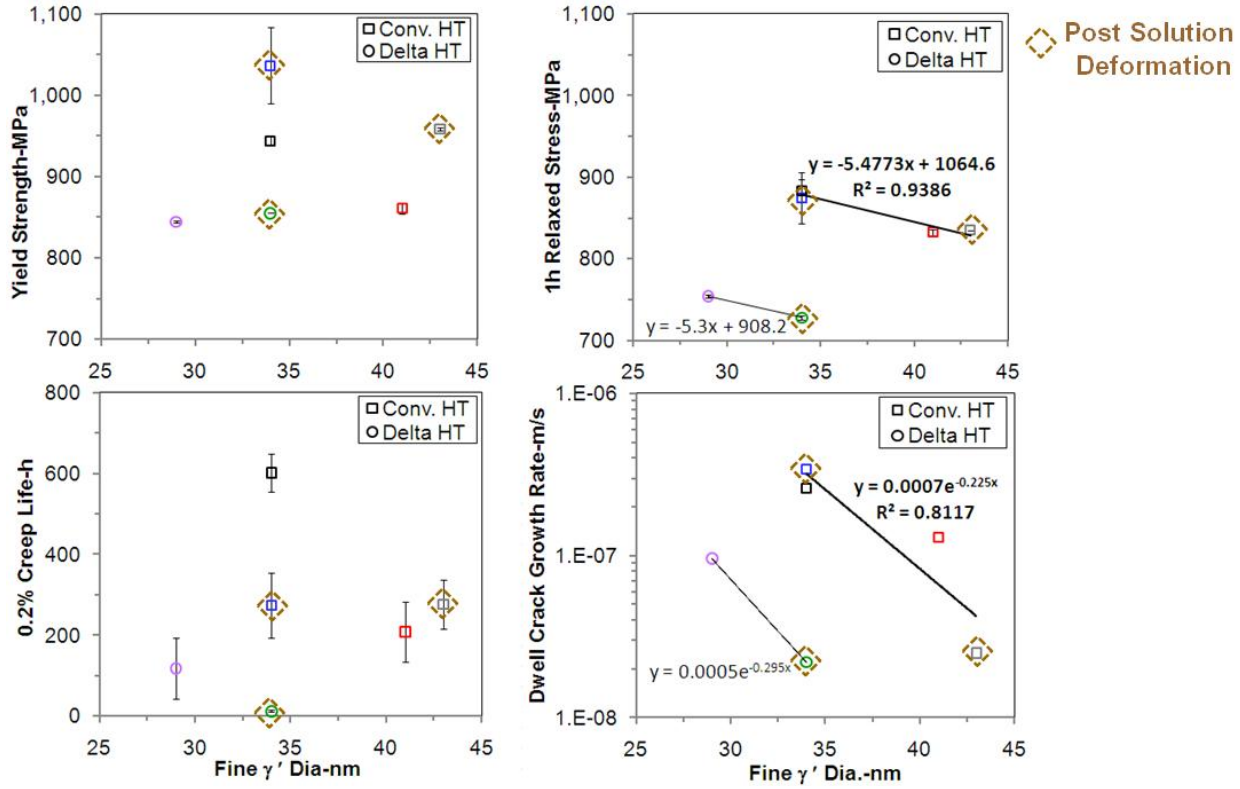

Figure 15.—Mechanical properties versus fine γ ′ size.

In the microstructure-property plots, conventional and δ heat treated conditions were considered separately. The coarse plates of δ phase may not contribute substantially to strength or creep resistance (Ref. 1). Therefore, the lower strengths of δ heat treated cases could be associated with the lower volume fractions and bimodal populations of γ′ precipitates observed here, and indicate that these properties as measured in the present test conditions were largely influenced by the γ′ precipitates through dislocation shearing and bypass mechanisms, respectively, rather than by grain boundary sliding. It is not clear what role was played by the very fine γ″ phase particles often attached to γ′ precipitates. However, the size of these particles did not seem to change among the different conditions, so their effects on mechanical properties could be similar for the six cases examined.

The δ heat treatment also produced lower dwell fatigue crack growth rates than for conventional heat treated material, accompanied by smaller proportions of intergranular cracking. The large reductions in relaxed stresses for δ heat treated materials could help explain this response, as the increase in stress relaxation can result in a decrease in the corresponding crack tip crack driving force which in turn would lower the dwell crack growth rates. These results are in agreement with previously reported data showing that heat treatments which produce extensive stress relaxation led to lower dwell crack growth rates for 718Plus (Ref. 20) and a powder metallurgy superalloy (Ref. 9). The presence of δ phase plates along many grain boundaries also may have influenced dwell crack growth rates by altering the intergranular damage and cracking process, to either improve (Ref. 20) or impair (Ref. 17) dwell crack growth resistance. Additional studies systematically varying δ phase content independently from mechanical properties would be necessary to fully separate and rank these influences on dwell fatigue crack growth rates.

The addition of GBE with post-solution deformation for δ heat treated material did not greatly affect strength and stress relaxation response, yet gave the lowest creep resistance and lowest dwell crack growth rates. So comparison of the NGD and GIPD cases can allow estimation of the effects of increased preferred grain boundary content on dwell crack growth, at nearly fixed strength and stress relaxation properties. This comparison indicates that preferred grain boundaries of the GIPD case gave a substantial benefit of near 5x to dwell crack growth rates, and reduced intergranular cracking. However, this case had slightly higher δ phase content and slightly larger mean size of fine γ′ precipitates. These differences as well as larger average grain size for GIPD could also contribute to the crack growth improvements.

Grain boundary engineering combined with post-solution deformation and conventional heat treatment enabled an increase in yield strength, combined with enhanced stress relaxation and primary creep. This allowed the GIIP condition to have a preferable combination of high yield strength, good creep resistance, and dwell crack growth resistance in the present study, as shown in Figure 16. This is an important and significant finding, since it leads to a favorable balance of high temperature mechanical properties, without the typical sacrifice in yield strength and creep resistance for improved dwell crack growth resistance.

It does not appear that the increased percentage of preferred grain boundaries produced by GBE alone could have provided this yield strength improvement. If that were the case, the GI condition would also have shown increased rather than reduced yield strength. Rather, the post- solution deformation after GBE appeared to provide much of the increase in yield strength, evident for the GIP and GIIP cases. This post-solution deformation produced many slip bands as shown in Figure 17, which could provide initial dislocation hardening but also facilitate through time-dependent dislocation rearrangement enhanced stress relaxation that was observed for these material conditions. In this respect, GBE with post-solution deformation may effectively operate as conventional cold work, which was previously shown to enhance yield strength yet increase stress relaxation in 718 (Ref. 21) and in powder metallurgy superalloys Rene′ 95 (Ref. 22) and IN100 (Ref. 23). These slip bands were not observed for the GIPD case, where the δ heat treatment of 930 °C/4 h apparently annealed out this plastic deformation, while preferentially precipitating δ plates on the slip bands.

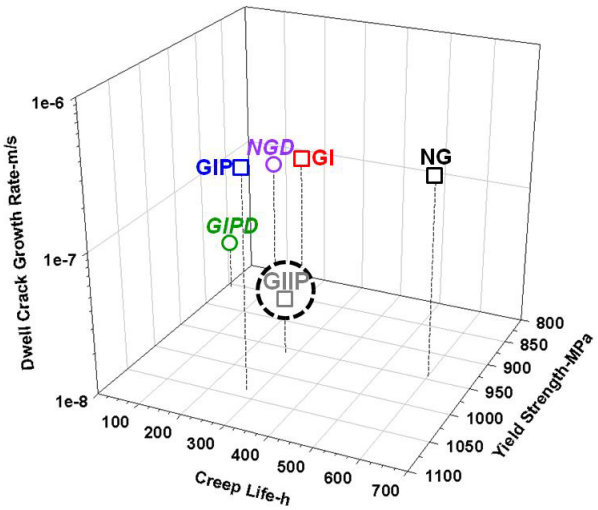

Figure 16.—Comparison of the trade in mechanical properties.

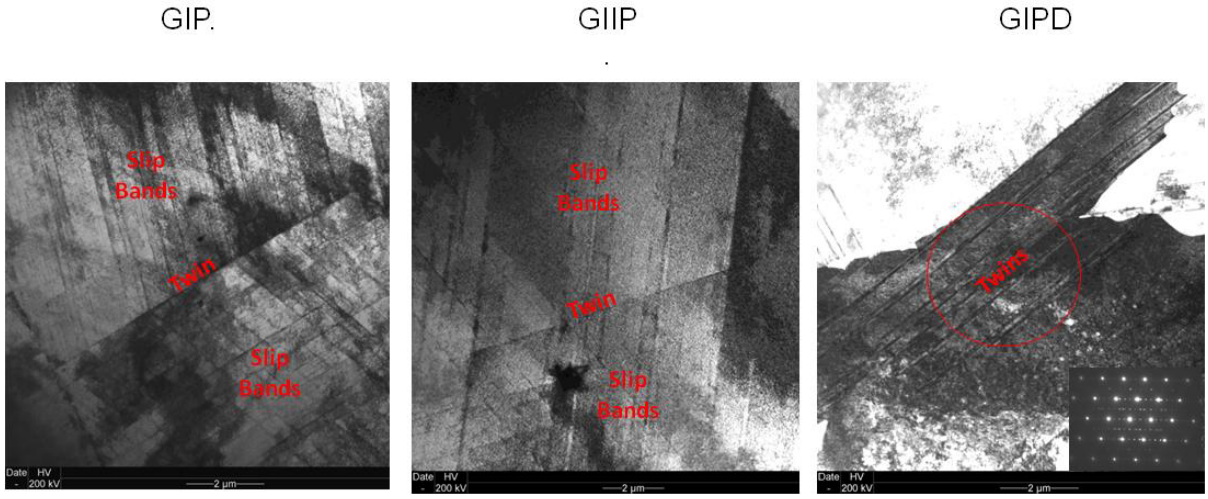

Figure 17.—Effects of post-solution deformation on microstructure.

The resulting dwell crack growth rates for conventional heat treated cases were sensitive to GBE processing. Application of GBEI processing before final solution heat treatment gave a modest reduction in dwell crack growth rates and intergranular cracking for the GI condition. Inclusion of a post-solution deformation step after this same GBEI processing eliminated this benefit for condition GIP. Yet, the enhanced GBEII process combined with post-solution deformation gave larger reductions in dwell crack growth rates and intergranular cracking, in the GIIP condition. The strengthening γ′ precipitate size consistently increased with decreasing crack growth rate for these cases, however, a single correlation between dwell fatigue crack growth and γ′ precipitate size did not appear to be governing for all cases, Figure 15. The additional effects of δ heat treatments and post solution deformation can explain this lack of a single correlation as observed elsewhere (Ref. 9).

Dwell fatigue crack growth is partly dependent on the connectivity of these high angle grain boundaries, and the "connectivity" of high angle boundaries was appreciably decreased by GBE (Ref. 14). But this was confounded by the effects of other changes in these microstructures which were previously described, and the associated changes in yield strength and stress relaxation that would affect both stresses and plastic/creep zone sizes at the crack tip. Yet, decreased connectivity of high angle grain boundaries in GBE materials probably contributed to the slower measured crack growth rates, reflected in

the comparison of NGD and GIPD responses. Additional, interrupted dwell crack growth tests and subsequent metallographic sectioning would help to further investigate these concepts.

In summary, these aspects suggest a generalized GBE microstructure-property framework and model to account for the results would require statistical evaluation of several terms: special grain boundary content (Fsp), grain size ($D^{-1/2}$), fine γ' size (d_f) and content (f_f). δ phase size (d_δ) and content (f_δ), and slip band or dislocation density (ρ). These terms could not be clearly evaluated with multiple linear regression for the six current conditions tested, due to confounded variations of several terms. One would need to systematically vary these terms in a matrix of statistically designed processing-microstructure cases, for proper evaluations.

Potential Future Work

Additional work could help to better understand and optimize microstructure-mechanical property relationships for grain boundary engineered materials. For the current material, additional, interrupted crack growth tests could allow better understanding of how dwell fatigue crack growth varied with material condition. Longitudinal sectioning could be used here to isolate crack paths, allow quantification of grain boundary character, connectivity, crystallographic orientation, and surrounding grain constraints necessary during fatigue crack growth. This could help allow identification of all influential microstructure variables. Additional material processing conditions could then be added, to systematically vary all relevant microstructure terms in a manner allowing unambiguous statistical evaluations. Predictive models relating GBE and post-solution deformation to microstructure and properties could then be generated.

Such knowledge could be applied to help guide optimal balancing of properties through GBE using the current approaches, as well as through other thermo-mechanical and surface treatment processes. Disk forging, surface shot peening, or low plasticity burnishing (Ref. 21) could be applied in attempts to replicate these effects on microstructure for similar enhancement of properties. Altered heat treatments with varied solution and aging times, temperatures, and paths could be applied to potentially further improve the balance of properties.

Summary and Conclusions

The influences of grain boundary engineering on the microstructures and high temperature mechanical properties of a disk superalloy were screened. Selected samples of 718Plus superalloy were given grain boundary engineering (GBE) treatments to increase the fraction of low CSL grain boundaries. Conventional and δ heat treatments were then consistently applied in samples with and without prior GBE processing. Mechanical properties were subsequently screened in tensile stress relaxation, creep, and dwell fatigue crack growth tests.

GBE before final solution and aging heat treatments reduced yield strength and creep resistance, yet also reduced the extent of stress relaxation. Dwell fatigue crack growth rates were modestly improved for this case. The δ heat treatment independently reduced yield strength and creep resistance, and increased stress relaxation over those properties for conventional heat treatment conditions. This gave moderately improved dwell crack growth rates.

GBE combined with a final cold rolling deformation step after solution heat treatment produced an advantageous balance of increased yield strength and reduced creep resistance, with increased stress relaxation. This could also reduce dwell fatigue crack growth rates. However, dwell crack growth rates appeared sensitive to variation of GBE processing. Combination of the GBEI process with post-solution deformation and δ heat treatment gave lowest dwell crack growth rates. This was correlated with a coarser, bimodal gamma prime size distribution promoted by the δ heat treatment, the presence of δ phase plates both within grains and at grain boundaries, and the increased twin and preferred grain boundary content promoted by GBE. This microstructure allowed the lowest proportion of intergranular cracking during dwell fatigue crack growth.

It can be concluded from this work that:

1. Allvac 718Plus microstructures and mechanical properties can be significantly influenced by grain boundary engineering.
2. The addition of a deformation step after final solution heat treatment can be used to alter the effects of grain boundary engineering.
3. These effects can be combined with a δ heat treatment to enhance dwell crack growth resistance and minimize intergranular cracking.
4. The combination of grain boundary engineering with post solution deformation and conventional aging can give a most favorable balance of strength, creep resistance, stress relaxation, and dwell fatigue crack growth resistance.

References

1. W.D. Cao and R.L. Kennedy, "Role of Chemistry in 718 Type Alloys–Allvac 718Plus™ Development," *Superalloys 2004*, ed. K.A. Green, H. Harada, T.E. Howson, T.M. Pollock, R.C. Reed, J.J. Schirra, S. Walston (Warrendale, PA: The Metallurgical Society of AIME, 2004), 91–99.
2. L. Pike, "Development of a Fabricable Gamma Prime (γ') Strengthened Superalloy," *Superalloys 2008*, ed. R.C. Reed, K.A. Green, P. Caron, T.P. Gabb, M.G. Fahrmann, E.S. Huron, S.A. Woodard, (Warrendale, PA: The Metallurgical Society of AIME, 2008), 191–200.
3. P.F. Browning, "Time Dependent Crack Tip Phenomena in Gas Turbine Disk Alloys," PhD Thesis, Rensellaer Polytechnique Institute, Troy, New York, 1998.
4. R. Molins, G. Hochstetter, E. Andrieu, "Oxidation Effects on the Fatigue Crack Growth Behaviour of Alloy 718 at High Temperature," *Acta. Mater*. 45 (1997), 663–674.
5. S. Everitt, M. Starink, and P. Reed, "Temperature and Dwell Dependence of Fatigue Crack Propagation in Various Heat Treated Turbine Disc Alloys," *Superalloys 2008*, ed. R.C. Reed, K.A. Green, P. Caron, T.P. Gabb, M.G. Fahrmann, E.S. Huron, S.A. Woodard, (Warrendale, PA: The Metallurgical Society of AIME, 2008), 741–752.
6. K.R. Bain, M.L. Gambone, J.M. Hyzak, and M.C. Thomas, "Development of Damage Tolerant Microstructures in UDIMET 720," *Superalloys 1988*, ed. D.N. Duhl, G. Maurer, S. Antolovich, C. Lund, and S. Reichman, (Warrendale, PA: The Metallurgical Society of AIME, 1988), 13–22.
7. J. Gayda, R.V. Miner, T.P. Gabb, "On the Fatigue Crack Propagation Behavior of Superalloys at Intermediate Temperatures," *Superalloys 1984*, ed. M. Gell, (Warrendale, PA: The Metallurgical Society of AIME, 1984), 731–740.
8. E.S. Huron, K.R. Bain, D.P. Mourer, J.J. Schirra, P.L. Reynolds, and E.E. Montero, "The Influence of Grain Boundary Elements on Properties and Microstructures of P/M Nickel Base Superalloys," *Superalloys 2004*, ed. K.A. Green, H. Harada, T.E. Howson, T.M. Pollock, R.C. Reed, J.J. Schirra, S. Walston, (Warrendale, PA: The Metallurgical Society of AIME, 2004), 73–82.
9. J. Telesman, T.P. Gabb, A. Garg, P. Bonacuse, J. Gayda, "Effect of Microstructure on Time Dependent Fatigue Crack Growth Behavior in a P/M Turbine Disk Alloy," *Superalloys 2008*, ed. R.C. Reed, K.A. Green, P. Caron, T.P. Gabb, M.G. Fahrmann, E.S. Huron, S.A. Woodard, (Warrendale, PA: The Metallurgical Society of AIME, 2008), 807–816.
10. T.P. Gabb, J. Gayda, J. Telesman, A. Garg, "The Effects of Heat Treatment and Microstructure Variations on Disk Superalloy Properties at High Temperature," *Superalloys 2008*, ed. R.C. Reed, K.A. Green, P. Caron, T.P. Gabb, M.G. Fahrmann, E.S. Huron, S.A. Woodard, (Warrendale, PA: The Metallurgical Society of AIME, 2008), 121–130.
11. V.B. Trindade, U. Krupp, Ph. E.-G. Wagenhuber, H.-J. Christ, "Oxidation Mechanisms of Cr-Containing Steels and Ni-base alloys at High Temperatures—Part I: The Different Role of Alloy Grain Boundaries," *Materials and Corrosion* 56 (2005) 785–790.

12. E.M. Lehockey, G. Palumbo, P. Lin, A.M. Brennenstuhl, "On the Relationship Between Grain Boundary Character Distribution and Intergranular Corrosion," *Scripta Materialia* 36 (1997) 1211–1218.
13. E.M. Lehockey, G. Palumbo, "On the Creep Behavior of Grain Boundary Engineered Nickel," *Materials Science and Engineering* A237 (1997) 168–162.
14. P. Lin, V. Provenzano, G. Palumbo, T.P. Gabb, J. Telesman, "Grain Boundary Engineering of Allvac 718Plus for Aerospace Engine Applications," *7th International Symposium on Superalloy 718 and Derivatives*, ed. E. Ott, J.R. Groh, A. Banik, X. Liu, R.C. Helmink, A. Mitchell, T.P. Gabb, A. Wusatowska-Sarnek, I. Dempster, G.P. Sjöberg, (Warrendale, PA: The Metallurgical Society of AIME, 2010).
15. R.H. Vanstone, T.L. Richardson, "Potential-Drop Monitoring of Cracks in Surface-Flawed Specimens," *ASTM STP 877*, (W. Conshohocken, PA: American Society for Testing and Materials, 1985) 148–166.
16. Y. Gao, M. Kumar, R.K. Nalla, R.O. Ritchie, "High-Cycle Fatigue of Nickel-Based Superalloy ME3 at Ambient and Elevated Temperatures: Role of Grain-Boundary Engineering," *Met. Trans. A* 36A (2005), 3325–3333.
17. K.A. Unocic, R.W. Hayes, M.J. Mills, G.S. Daehn, "Microstructural Features Leading to Enhanced Resistance to Grain Boundary Creep Cracking in Allvac 718Plus," *Met. Trans. A*, 41A (2010), 409–420.
18. J.A. Manriquez, P.L. Bretz, L. Rabenberg, J.K. Tien, "The High Temperature Stability of IN718 Derivative Alloys," *Superalloys 1992*, ed. S.K. Antolovbich, R.W. Stusrud, R.A. MacKay, D.L. Anton, T. Khan, R.D. Kissinger, D.L. Klarstrom, (Warrendale, PA: The Metallurgical Society of AIME, 1992), 507–516.
19. F. Taina, M. Pasqualon, V. Velay, D. Delagnes, P. Lours, "Effect of the LCF Loading Cycle Characteristics on the Fatigue Life of Inconel 718 at High Temperature," *7th International Symposium on Superalloy 718 and Derivatives*, ed. E. Ott, J.R. Groh, A. Banik, X. Liu, R.C. Helmink, A. Mitchell, T.P. Gabb, A. Wusatowska-Sarnek, I. Dempster, G.P. Sjöberg, (Warrendale, PA: The Metallurgical Society of AIME, 2010).
20. X. Liu, J. Xu, E. Barbero, W.D. Cao, R.L. Kennedy, "Effect of Thermal Treatment on the Fatigue Crack Propagation Behavior of a New Ni-base Superalloy," *Mat. Sci. Eng.* 474 (2008), 30–38.
21. P. Prevey, R.A. Ravindranath, M.J. Shepard, T.P. Gabb, "Case Studies of Fatigue Life Improvement Using Low Plasticity Burnishing in Gas Turbine Engine Applications," *Proceedings of ASME Turbo Expo 2003*, ASME, June, 2003.
22. T.P. Gabb, J. Telesman, P.T. Kantzos, P.J. Bonacuse, R.L. Barrie, and D.J. Hornbach, "Stress Relaxation in Powder Metallurgy Superalloy Disks," *TMS Letters* 5 (2004), 115–116.
23. D. Buchanan, R. John, R. Brockman, and A. Rosenberger, "A Coupled Creep Plasticity Model for Residual Stress Relaxation of a Shot Peened Nickel-Base Superalloy," *Superalloys 2008*, ed. R.C. Reed, K.A. Green, P. Caron, T.P. Gabb, M.G. Fahrmann, E.S. Huron, S.A. Woodard, (Warrendale, PA: The Metallurgical Society of AIME, 2008), 965–974.

REPORT DOCUMENTATION PAGE	Form Approved OMB No. 0704-0188

1. REPORT DATE *(DD-MM-YYYY)*	2. REPORT TYPE	3. DATES COVERED *(From - To)*
01-12-2010	Technical Memorandum	

4. TITLE AND SUBTITLE
Grain Boundary Engineering the Mechanical Properties of Allvac 718Plus™ Superalloy

5a. CONTRACT NUMBER

5b. GRANT NUMBER

5c. PROGRAM ELEMENT NUMBER

6. AUTHOR(S)
Gabb, Timothy, P.; Telesman, Jack; Garg, Anita; Lin, Peter; Provenzano, Virgil; Heard, Robert; Miller, Herbert, M.

5d. PROJECT NUMBER

5e. TASK NUMBER

5f. WORK UNIT NUMBER
WBS 698259.02.07.03.04.02

7. PERFORMING ORGANIZATION NAME(S) AND ADDRESS(ES)
National Aeronautics and Space Administration
John H. Glenn Research Center at Lewis Field
Cleveland, Ohio 44135-3191

8. PERFORMING ORGANIZATION REPORT NUMBER
E-17539

9. SPONSORING/MONITORING AGENCY NAME(S) AND ADDRESS(ES)
National Aeronautics and Space Administration
Washington, DC 20546-0001

10. SPONSORING/MONITOR'S ACRONYM(S)
NASA

11. SPONSORING/MONITORING REPORT NUMBER
NASA/TM-2010-216935

12. DISTRIBUTION/AVAILABILITY STATEMENT
Unclassified-Unlimited
Subject Category: 07
Available electronically at http://gltrs.grc.nasa.gov
This publication is available from the NASA Center for AeroSpace Information, 443-757-5802

13. SUPPLEMENTARY NOTES

14. ABSTRACT
Grain Boundary Engineering can enhance the population of structurally-ordered "low S" Coincidence Site Lattice (CSL) grain boundaries in the microstructure. In some alloys, these "special" grain boundaries have been reported to improve overall resistance to corrosion, oxidation, and creep resistance. Such improvements could be quite beneficial for superalloys, especially in conditions which encourage damage and cracking at grain boundaries. Therefore, the effects of GBE processing on high-temperature mechanical properties of the cast and wrought superalloy Allvac 718Plus (Allvac ATI) were screened. Bar sections were subjected to varied GBE processing, and then consistently heat treated, machined, and tested at 650 °C. Creep, tensile stress relaxation, and dwell fatigue crack growth tests were performed. The influences of GBE processing on microstructure, mechanical properties, and associated failure modes are discussed.

15. SUBJECT TERMS
Gas turbine engines; Rotating disks; Heat resistant alloys

16. SECURITY CLASSIFICATION OF:			17. LIMITATION OF ABSTRACT	18. NUMBER OF PAGES	19a. NAME OF RESPONSIBLE PERSON
a. REPORT	b. ABSTRACT	c. THIS PAGE			STI Help Desk (email:help@sti.nasa.gov)
U	U	U	UU	25	19b. TELEPHONE NUMBER *(include area code)* 443-757-5802